Impervious Surface Extraction Based on Improved Support Vector Data Description

Yuwen Fei
School of Geographic Sciences, Hunan Normal University, Changsha 410081, China.

Abstract: The continuous expansion of urban impervious surfaces has brought negative impacts on the urban environment. In order to quickly extract urban impervious surfaces to monitor urban development, this paper proposes a multiresolution segmentation-based impervious surface extraction method. The method is an improvement on the deep support vector data description method. The study is carried out to validate the method using some areas of Shenzhen as the experimental area. The experimental results show that the improved DSVDD method has enhanced all accuracy indicators, while its landscape pattern index reflects that the improved model has less fragmentation.
Keywords: Impervious Surface; Support Vector Data Description; Multiresolution Segmentation; Remote Sensing Images

1. Introduction

Impervious surface refers to the type of surface that hinders water infiltration such as asphalt, cement, etc. Urban impervious surface mainly covers roads, squares and other transportation facilities and construction facilities[1]. The gradual increase in the percentage of impervious surface in cities will lead to urban flooding, urban heat island and many other urban problems. Therefore, the extraction of impervious surfaces in cities has received much attention. One-class classification algorithms are often used in the case of one-class training samples, and Miao et al[2] and Wan et al[3] performed impervious surface extraction studies using one-class classification methods. Meanwhile, multiresolution segmentation methods are often used to process samples. But few people make use of multiresolution segmentation results to improve on one-class classification methods. In this paper, an improved support vector data description method is proposed based on this.

2. Study Area

Shenzhen is one of the cities with the fastest urbanization process and has typical urbanization characteristics. In this paper, the area of 113.95°E -114.04°E longitude and 22.73°N -22.64°N latitude in Shenzhen is selected as a typical experimental area, which contains typical features such as housing buildings, urban roads and parks and green areas.

3. Methodology

3.1 Sample production for the study

The Gaofen-1 image was used as the base remote sensing image, and OSM road data, OSM building data, vehicle trajectory data and POI data, were collected to obtain the distribution locations of urban impervious surfaces (all of the above data are taken from 2018, and the data distribution is shown in Figure 1). Most of the above four types of geographic data are generated on the urban impervious surface, therefore the higher the frequency of geographic data generation in an area, the higher the probability of it being impervious. For this reason, this study obtains urban impervious surface coverage samples by the location of geographic data generation.

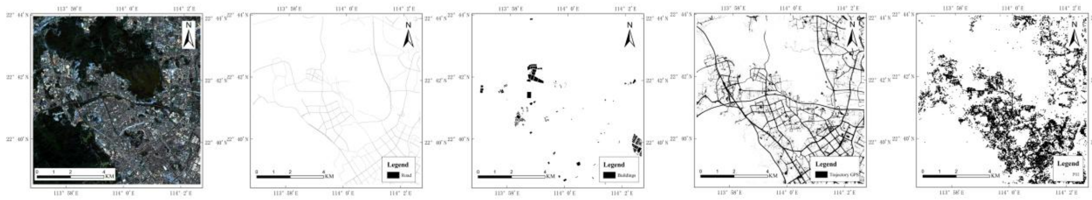

(a) (b) (c) (d) (e)

Figure 1 Research data (a) remote sensing image (b) OSM road data (c) OSM building data (d) vehicle trajectory data (e) POI data

3.2 One-class algorithm model construction

The deep support vector data description (DSVDD) is selected for constructing the impervious surface extraction model. DSVDD minimizes the objective function with the help of a neural network, so that the optimal hypersphere is found in the hypersphere space to fit all training samples, and finally the target class is distinguished from the non-target sample class. The objective function is as follows.

$$\min_{R,\mathcal{W}} R^2 + \frac{1}{\upsilon n}\sum_{i=1}^{n} max\{0, \| \phi(x_i;\mathcal{W}) - c \|^2 - R^2\} + \frac{\lambda}{2}\sum_{l=1}^{L} \| W^l \|_F^2 \ (1)$$

where the radius R, the center of the sphere c to determine the location of the hypersphere in space. n is the number of training samples and $\upsilon \in [0,1]$ is used to control the trade-off between the hypersphere volume and the boundary. $\phi(x_i;\mathcal{W})$ denotes the mapping of the sample x_i through the neural network, which has a weight matrix of W. $\frac{\lambda}{2}\sum_{l=1}^{L} \| W^l \|_F^2$ is employed to constrain the neural network to prevent overfitting.

The trained model is used for the classification of the samples to be tested. By determining the position of the sample in relation to the optimal hypersphere, it is possible to determine whether the sample is a target class, i.e., a sample falling inside the sphere is defined as a target class, and a sample falling outside the sphere is defined as a non-target class. The position determination function of the test sample and the optimal hypersphere can be shown as follows.

$$S(x_i) = \| \phi(x_i;\mathcal{W}^*) - c \|^2 - R^{*2} (2)$$

where $S(x_i)$ is the position determination function, $\phi(x_i;\mathcal{W}^*)$ denotes the trained mapping network model, and c and R^* are the center and radius of the optimal hypersphere, respectively.

3.3 Optimization based on multiresolution segmentation

Affected by machine algorithm misclassification and data noise, a complete geographic object is sometimes predicted as multiple sample categories. Considering that the same geospatial object should have consistent category labels, this study optimizes the classification results of DSVDD based on the idea of spatial statistics and with the help of multiresolution segmentation results. The experiments were performed by eCognition9.0 for multiresolution segmentation of images, which is a bottom-up segmentation algorithm based on a pairwise region merging technique that successively merges pixels or existing image objects[4].

4. Results

In this study, the multiresolution segmentation results are used to optimize the DSVDD results, so as to construct an improved DSVDD method. In order to evaluate the impervious surface extraction performance of the improved method, the results are statistically analyzed experimentally in two dimensions: accuracy assessment index and landscape pattern index.

TP, TN, FP, and FN were used to denote the number of true positive, true negative, false positive, false negative, and positive class samples in the confusion matrix, respectively. N denotes the number of all patches, and A and E denote the total area of impervious surface and the total perimeter of the boundary, respectively. The evaluation indexes were calculated as in Table 1.

Table 1 Calculation method of evaluation indicators

Indicators	Calculation formula
Overall accuracy (OA)	$OA = \frac{TP + TN}{TP + TN + FP + FN}$
Precision	$P = \frac{TP}{TP + FP}$
Recall	$R = \frac{TP}{TP + FN}$
F1-score	$F = \frac{2TP}{2TP + FP + FN}$
Landscape fragmentation (LF)	$LF = \frac{NP}{A}$
Edge Density (ED)	$ED = \frac{E}{A}$
Landscape Shape Index (LSI)	$LSI = \frac{0.25E}{\sqrt{A}}$

The experiment first uses eCognition to perform multiresolution segmentation of the images (Figure 2(a)), and then optimizes the classification results of DSVDD based on the segmented images. 10,000 test points were selected to show the accuracy of impervious surface extraction before and after the model improvement, and the specific accuracy performance and classification result plots are shown in Table 2 and Figure 2, respectively. The results show that the OA of the improved DSVDD method is improved from 86.95% to 87.38%, and its Recall, Precision and F1-score metrics are also slightly improved. Comparing Figure. 2(b) and Figure. 2(c), it can also be found that the improved method can reduce the pretzel noise problem in the classification and can better fit the impervious surface boundary location.

Table 2 Comparison of extraction accuracy of impervious surface

Method	Recall	Precision	OA	F1-score
DSVDD	91.03%	84.22%	86.95%	87.45%
Improved DSVDD	91.24%	84.84%	87.38%	87.89%

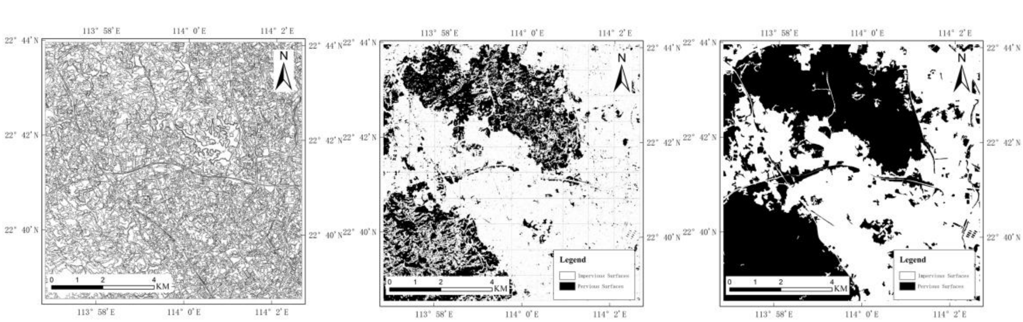

(a) (b) (c)

Figure 2 Experimental result graph (a) multiresolution segmentation results (b) impervious surface extraction results with DSVDD (c) impervious surface extraction results with improved DSVDD

Landscape fragmentation reflects the spatial complexity of the landscape and the degree of human interference with the landscape[5]. Higher landscape fragmentation and more number of patches both reflect higher fragmentation. The landscape shape index reflects the regularity of the patch shape, and the higher the index value when it is more irregular. Edge density represents the degree of connectivity of the landscape, the smaller the value, the better the connectivity. The impervious surface area is a typical man-made landscape, and the landscape pattern index can be used to reflect its spatial configuration and structural composition characteristics. Table 3 shows a comparison of the landscape pattern index performance of the two model approaches, and the results show that the extraction results have smaller landscape pattern index values using the improved DSVDD, which has less landscape fragmentation. This shows that the improved DSVDD method can supplement the information of details lost in model prediction due to misclassification and can better correct the boundary information of impervious surface.

Table 3 Comparison of the results of landscape pattern indicators

Method	Number of patches	LF	LSI	ED
DSVDD	120778	1.81	0.35	1.40
Improved DSVDD	315	1.04	0.24	0.96

5. Conclusion

Based on the background of rapid urbanization and gradual deterioration of urban environment, the expansion of impervious surface has become a hot topic of concern. In this study, the DSVDD method is improved based on the multiresolution segmentation results, and the superiority of the improved method is demonstrated in terms of both accuracy assessment index and landscape pattern index.

6. Acknowledgment

This work is supported by Postgraduate Scientific Research Innovation Project of Hunan Province, China (grant number: CX20210477).

References

[1] Wu C, Murray A T. Estimating impervious surface distribution by spectral mixture analysis[J]. Remote Sensing of Environment, 2003, 84(4): 493-505.

[2] Miao Z, Xiao Y, Shi W, et al. Integration of satellite images and open data for impervious surface classification[J]. IEEE Journal of Selected Topics in Applied Earth Observations and Remote Sensing, 2019, 12(4): 1120–1133.

[3] Wan Y, Fei Y, Wu T, et al. A novel impervious surface extraction method integrating poi, vehicle trajectories, and satellite imagery[J]. Ieee Journal of Selected Topics in Applied Earth Observations and Remote Sensing, 2021, 14: 8804–8814.

[4] eCognition Developer. eCognition Developer 9.0:Reference Book [M]. Munich, Germany: Trimble Germany GmbH,2014:35-40

[5] Chen C, Wu S, Meurk C, et al. Identifying and Evaluating Functional Connectivity for Building Urban Ecological Networks[J]. Acta Ecologica Sinica, 2015, 35(22):7367-7376.